

*The Crystal Structure of the Heusler Alloys.*

By A. J. BRADLEY, D.Sc., Royal Society Warren Research Fellow,  
and J. W. RODGERS, B.Sc.

(Communicated by W. L. Bragg, F.R.S.—Received October 4, 1933.)

Beginning in the year 1898 Heusler\* discovered a series of ferromagnetic alloys, the most important containing copper, manganese, and aluminium. They are characterized by remarkable magnetic properties, because although composed only of paramagnetic or diamagnetic elements, they become ferromagnetic after suitable heat treatment.† Various explanations of this property have been advanced, but it was usually considered to be due to the formation of a series of solid solutions of the type  $(\text{CuMn})_3\text{Al}$ , in which the proportions of copper and manganese may be varied within fairly wide limits.

The Heusler alloys have been repeatedly investigated by means of X-rays. Young,‡ using molybdenum radiation examined alloys of two different compositions. He found that one was face-centred cubic, while the other was a mixture of face-centred and body-centred cubic structures. The mixed alloy was the more magnetic.

A more detailed investigation was made by Leiv Harang,§ using copper radiation. He found three structures, face-centred cubic, body-centred cubic, and a structure similar to that of  $\gamma$  brass, which correspond respectively to the  $\alpha$ ,  $\beta$ , and  $\delta$  phases of the copper-aluminium system.|| They are successively produced by increasing the proportion of aluminium in the alloy. Harang did not find it possible to trace any relation between the magnetic properties and the crystal structure, and therefore could not ascribe them to a single lattice. These conclusions are not in agreement with recent investigations.¶

Later, Elis Persson investigated these alloys by means of chromium radiation. In a preliminary note\*\* he showed that the structure of a ferromagnetic alloy

\* Heusler, Stark, and Haupt, 'Verh. deuts. phys. Ges.,' vol. 5, p. 219 (1903); Heusler and Richarz, 'Z. anorg. Chem.,' vol. 61, p. 269 (1908).

† Take, 'Inaug. disc. Marburg' (1904).

‡ 'Phil. Mag.,' vol. 46, p. 291 (1923).

§ 'Z. Kristallog.,' vol. 65, p. 261 (1927).

|| Jette, Westgren, and Phragmén, 'J. Inst. Metals,' vol. 31, p. 201 (1924); Obinata, 'Mem. Ryojun Coll. Eng.,' vol. 31, pp. 3, 286, 295 (1929); Bradley and Jones, 'J. Inst. Metals,' vol. 51, p. 131 (1933).

¶ Krings and Ostmann, 'Z. anorg. Chem.,' vol. 163, p. 154 (1927); Heusler, 'Z. anorg. Chem.,' vol. 171, p. 126 (1928).

\*\* 'Naturwiss.,' vol. 16, p. 613 (1928).

corresponding to the formula  $\text{Cu}_2\text{MnAl}$  was body-centred cubic, with the aluminium atoms forming a face-centred superlattice. The structure was therefore like that of  $\text{Fe}_3\text{Si}$ \*, or that of  $\text{Fe}_3\text{Al}$ † discovered later. The unit cell is built up of eight small body-centred cubes, and therefore contains 16 atoms, of which four are aluminium, four manganese, and the remainder copper. The aluminium atoms form a face-centred cube with double the dimensions of the small body-centred cube. No attempt was made to find the position of the manganese atoms by means of X-rays.

Potter‡ made an X-ray examination of single crystals using copper radiation. He believed that the Mn atoms occupied special positions like the Al atoms. On account of the resemblance between the magnetic properties of this alloy and nickel, he concluded that its ferromagnetism was due to the manganese atoms being arranged on a face-centred cubic lattice.

In continuation of his earlier researches, Persson§ came to the same conclusion. The series of alloys  $(\text{CuMn})_3\text{Al}$  is only ferromagnetic when the manganese content exceeds 19% (atomic). This is independent of the arrangement of aluminium atoms, which is apparently the same whatever the amount of manganese present, within wide limits. Persson believes that the presence of 19% of manganese is required in order to produce a regular arrangement of manganese atoms.

Persson attempted to find whether the special  $\text{Cu}_2\text{MnAl}$  type of structure was alone responsible for the ferromagnetic properties of the copper-manganese-aluminium alloys. He examined a whole series of alloys of the composition  $(\text{CuMn})_3\text{Al}$ , varying the proportions of copper and manganese. An X-ray examination was made after heat treatment of the powdered alloy. In one series of experiments the alloys were quenched in water from a temperature only  $50^\circ$  below the melting point. In another series the alloys were tempered for 350 hours at  $210^\circ$ .

The quenching experiments showed that four different types of structure occurred. Face-centred cubic, body-centred cubic, and "Gamma" structures corresponded to the  $\alpha$ ,  $\beta$  and  $\delta$  phases of the copper-aluminium system, and a fourth phase possessed a structure like that of  $\beta$  Mn. Contrary to Harang, Persson concluded that only the body-centred cubic  $\beta$  phase was ferromagnetic, the ferromagnetism of the alloys increasing with the amount of the  $\beta$  phase present.

\* Phragmén, 'Tekn. Tidskrift' (Stockholm), vol. 56, p. 81 (1926)

† Bradley and Jay, 'Proc. Roy. Soc.,' A, vol. 136, p. 210 (1932).

‡ 'Proc. Phys. Soc.,' London, vol. 41, p. 135 (1929).

§ 'Z. Physik,' vol. 57, p. 115 (1929).



The tempering experiments showed that the  $\beta$  phase was decomposed by this form of heat treatment. The alloy splits up into two or more phases. If the Mn content is less than required for the formation of the alloy  $\text{Cu}_2\text{MnAl}$ , the phases are  $\text{Cu}_3\text{Al}$  with lattice spacing 5.833 A., and  $\text{Cu}_2\text{MnAl}$  with lattice spacing 5.950 A. If the Mn content is greater, a structure of the  $\beta$  Mn type with lattice spacing 6.370 A. is formed, together with  $\text{Cu}_2\text{MnAl}$  with lattice spacing 5.950 A. Maximum ferromagnetism corresponds to the greatest amount of  $\text{Cu}_2\text{MnAl}$ .

Whether the alloy is quenched or tempered the lattice spacing of the  $\beta$  body-centred cubic phase never exceeds 5.950 A. For quenched alloys the lattice spacing increases linearly with increase of manganese content between  $\text{Cu}_3\text{Al}$  and  $\text{Cu}_2\text{MnAl}$  and ferromagnetism is the greater the greater the lattice spacing.

An alloy of the composition  $\text{CuMnAl}_2$  has the CsCl type of structure and is non-magnetic. The property of ferromagnetism is thus associated in a peculiar degree with the special composition  $\text{Cu}_2\text{MnAl}$ . The closer the alloy attains to this composition the more marked is its ferromagnetic character. Persson concludes that the property of ferromagnetism is due to the nature of the crystal structure of  $\text{Cu}_2\text{MnAl}$ , and is linked up with the mode of distribution of the manganese atoms.

The object of the present paper is to fix the position of the manganese atoms in the magnetic alloys by direct experiment, and to test whether a change of structure *without change of composition* will destroy the ferromagnetic character of the alloy. This should decide whether structure or composition is the more important condition for ferromagnetism.

### I. Present Experiments.

Eight alloys of the approximate composition  $\text{Cu}_2\text{MnAl}$  were prepared by melting together 50 gm. of copper, manganese, and aluminium in slightly different proportions in an alumina lined crucible\* in a high frequency induction furnace, under a low pressure of hydrogen. In order to remove coring, and to make the alloys homogeneous, they were heated for 6 hours at 750° C. in an electric furnace and allowed to cool slowly down to room temperature. Drillings were then taken by means of a special drill,† kindly supplied by Mr. Gardiner, of Easterbrook Allcard & Co., Sheffield. The drillings gave small particles which could be ground in an agate mortar. The fine powders so obtained were

\* Jay, 'J. Iron and Steel Inst.,' vol. 125, p. 427 (1932).

† Edgar Allen's Stag Major.

sieved through a mesh 250 to the inch, and then subjected to further heat treatment.

A portion was heated in hydrogen at 500° C. for 6 hours, and then allowed to cool slowly down to 300° C. over a period of a few hours. At this point the current was switched off, and the powders were allowed to cool to room temperature in the furnace. X-ray powder photographs of these alloys were taken using radiation from an iron anticathode. They show that the bulk of each alloy consists of a phase of the  $\gamma$  brass type\* like  $\text{Cu}_3\text{Al}_4$ † and that at least one other phase is present.

Very different photographs were obtained from the second portions of the powders. These were heated in hydrogen to a temperature of 800° C. and after about half an hour quenched by allowing a stream of cold water under pressure to enter the furnace. The structure is now body-centred cubic with superlattice of the typical Heusler alloy type, as described by Persson and Götter. These photographs were repeated using radiation from copper and from zinc anticathodes. There are differences between the relative intensities of the fainter lines of the three photographs, which we shall explain later.

In the alloy selected for detailed investigation the proportions of the ingredients did not correspond exactly to the theoretical values for the composition  $\text{Cu}_2\text{MnAl}$ . Analysis‡ of the alloy showed that the approximate composition was Cu 67.5%, Mn 17.5%, Al 15% corresponding to the atomic composition Cu 2.2, Mn 0.65, Al 1.15. The deficit of manganese was therefore made up partly by copper and partly by aluminium. This particular alloy was chosen because it was the only one which showed an almost complete change of structure with the two methods of heat treatment. After annealing at 500° and slowly cooling down to room temperature, it gave an X-ray powder photograph corresponding to the  $\delta$  copper aluminium structure ( $\text{Cu}_9\text{Al}_4$ ), with only a faint trace of lines belonging to another pattern. In this state the alloy was found to be practically non-magnetic. On the other hand, the same powder after quenching from 800° showed only a body-centred cubic structure with face-centred superlattice. The alloy was now strongly ferromagnetic.

\* Westgren and Phragmén, 'Phil. Mag.', vol. 50, p. 331 (1925); Bradley and Thewlis, 'Proc. Roy. Soc.', A, vol. 112, p. 678 (1926).

† Bradley, 'Phil. Mag.', vol. 6, p. 878 (1928); Bradley and Jones, 'J. Inst. Metals,' vol. 51, p. 131 (1933).

‡ The alloys were analysed by Mr. J. W. Cuthbertson of the University, to whom the authors are indebted for his kindness.



The above facts show conclusively that the magnetic properties of the alloy are dependent on the type of crystal structure, as Persson suggested. The composition of the alloy after heat treatment was checked by chemical analysis, and found to be unaltered.\* There is therefore no doubt that the ferromagnetism of the alloy is not a matter of chemical composition but of atomic arrangement.

The arrangement of the atoms in the annealed and slowly cooled alloy can be fixed to some extent from a visual inspection of the photograph. Its resemblance to the powder photograph of  $\text{Cu}_9\text{Al}_4$  is extraordinarily close. In  $\text{Cu}_9\text{Al}_4$ , the unit cell is cubic and contains 52 atoms of which 36 are copper

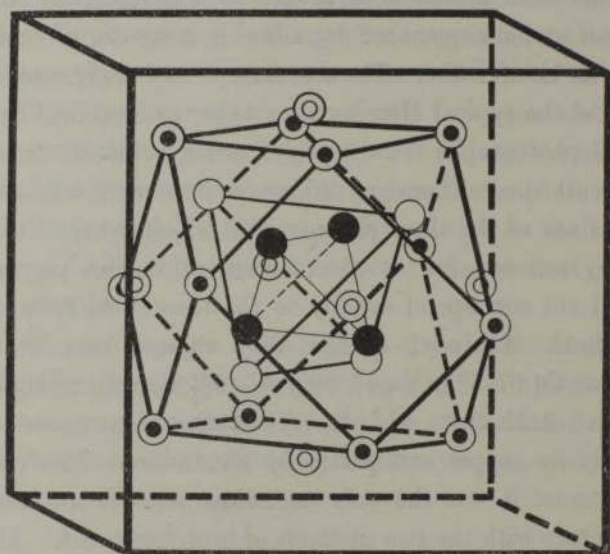


FIG. 1.—Annealed Heusler alloy (non-magnetic); ● A, ○ B, ⊙ C, ⊙ D.

and 16 aluminium. The copper and aluminium atoms each occupy definite positions in the lattice. From considerations of symmetry the 52 atoms can be divided into eight sets which may be called  $A_1, A_2; B_1, B_2; C_1, C_2; D_1, D_2$  respectively. Four  $A_1, 4 B_1, 6 C_1,$  and 12  $D_1$  constitute a cluster of 26 atoms which are grouped symmetrically around the centre of the unit cell, fig. 1. A second cluster of 26 atoms, not shown in the figure, is grouped symmetrically about each corner of the cell, so that the whole structure would be body-centred cubic, except for the fact that there are more copper atoms and fewer aluminium atoms in one cluster than in the other. The aluminium atoms are concentrated in  $A_1$  and  $D_2$ . The copper atoms occupy the remaining positions.

\* The manganese contents of the quenched and annealed specimens agreed to 0.1%.

The similarity of the powder photographs of the annealed Heusler alloy and that of  $\text{Cu}_9\text{Al}_4$  shows at once that the atomic co-ordinates are almost identical in the two. Further, it can be concluded that the aluminium atoms again occupy positions  $A_1$  and  $D_2$ . The remaining positions are filled chiefly by copper atoms, but about one-fourth of these are replaced by manganese. The formula of the annealed alloy can therefore be written as  $(\text{CuMn})_9\text{Al}_4$ . The proportions of aluminium are not quite sufficient to satisfy this formula, which may possibly explain the slight admixture of the second phase, shown by the powder photograph. Without a more detailed investigation, it is impossible to say whether the manganese atoms occupy special positions in the lattice, or whether they are mixed up with the copper atoms in a purely random manner, but there is no doubt about the aluminium atoms.

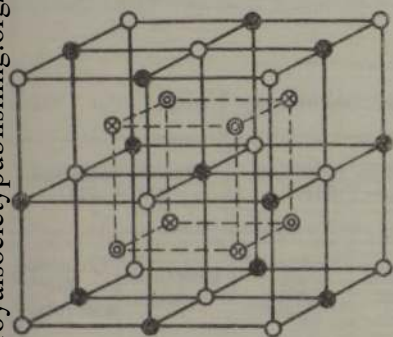


FIG. 2.—General type of structure;  
○ A, ⊙ B, ● C, ⊗ D.

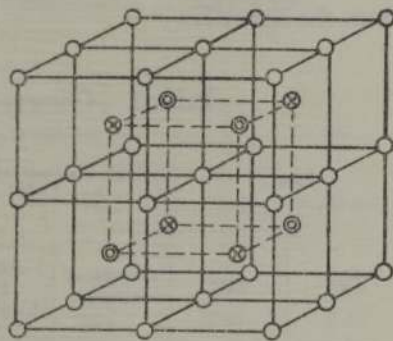


FIG. 3.—Quenched Heusler alloy (magnetic); ○ Cu, ⊙ Al, ⊗ Mn.

The ferromagnetic quenched alloy has a unit cell containing 16 atoms, fig. 2. These consist of four sets of atoms (A, B, C, D) each corresponding to a face-centred cubic lattice. The superlattice lines are caused by the segregation of the aluminium atoms into one of the four sets of positions (say B). Both Persson and Potter suggest that the ferromagnetism of these alloys is due to the manganese atoms occupying a special position as in fig. 3. It was our object to test this hypothesis. The question is whether the manganese atoms are mixed up at random with the copper atoms or whether they keep to their own positions. The difference between the scattering powers of copper and manganese for X-rays is so slight that this might at first sight appear to be a matter of some difficulty, but, in fact, the problem has been solved by means of accurate photometer measurements of powder photographs taken with X-rays of different wave-lengths, making use of the anomalies in atomic scattering



factor which occur when the frequency of the radiation is close to the characteristic absorption frequency of the element.

The powder photographs of the quenched alloys taken with iron, copper, and zinc radiations were photometered by means of a Cambridge micro-photometer. This instrument employs a null method, the blackening of the film being balanced against an Ilford wedge. Each film was calibrated by means of a rotating sector wheel, giving 10 uniform increments of intensity. On comparing the blackening of the film corresponding to each of the 10 steps, it is possible to trace the relationship between intensity and blackness characteristic of the film. For the films used in the present series of experiments the blackening curve is practically linear, so that the wedge readings may be taken as true measures of the intensity, some slight correction being applied to the strongest peaks where the calibration curve shows a slight departure from the linear law.

Table I.—Observed Intensities. Arbitrary Units.

Line.		Iron $K_{\alpha}$ radiation. $\lambda = 1.934$ .		Copper $K_{\alpha}$ radiation. $\lambda = 1.539$ .		Zinc $K_{\alpha}$ radiation. $\lambda = 1.434$ .	
$\Sigma h^2$ .	$hkl$ .	Observed values.	Corrected for absorption.	Observed values.	Corrected for absorption.	Observed values.	Corrected for absorption.
3	111	110	96	119	171	123	158
4	200	330	236	172	198	152	161
8	220	4730	2040	4041	2750	3663	2490
11	311	78	26	92	48.5	67	36
12	222	171	53	71	34.5	49	24
16	400	1181	288	895	342	758	303
19	331	31	6.5	47	15.5	29	10
20	420	272	54	111	35	53	18
24	422	3974	694	2111	503	1616	462
27	{ 511 } 333	58	8.5	35	8.5	43	11
32	440	2811	349	697	142	497	111
35	531	106	12	47	9	—	—
36	{ 600 } 442	867	94.5	62	11	—	—

For each line wedge readings were taken at intervals of 0.1 mm., and the blackening values so found plotted against the distance along the film. The areas included under the peak curve and above the general level of the background intensity were computed, and tabulated in Table I. Corrections for the effect of absorption in the powder specimen were made by the method

of graphical integration described by Claassen.\* The values of the absorption factor depend on the product of the absorption coefficient ( $\mu$ ) and the radius of the specimen ( $r$ ).

As a convenient method of support during the exposure, the specimen is diluted with Canada balsam and mounted on a hair. The effective value of  $\mu r$  is thereby reduced. The appropriate value of  $\mu r$  is most easily obtained from the following equation:—

$$\mu r = \frac{\mu}{\rho} m \frac{1}{\pi r l}$$

The weight of the specimen ( $m$ ) was 0.0024 gm., the length ( $l$ ) 0.49 cm., and radius ( $r$ ) 0.0265 cm. The values of  $\mu/\rho$  were calculated with the help of Jönsson's tables,† for each of the elements Al, Cu, and Mn with each of the radiations Fe, Cu, and Zn. The results are summarized in Table II.

Table II.

Radiation.	$\lambda$ .	$\mu/\rho$ values.				$\mu r$ .
		Al.	Cu.	Mn.	$\text{Cu}_2\text{MnAl}$ .	$\text{Cu}_2\text{MnAl}$ .
Fe $K_\alpha$ .....	1.934	93.9	100	64	89.5	5.3
Cu $K_\alpha$ .....	1.539	51.2	50.4	285	113	6.7
Zn $K_\alpha$ .....	1.434	41.8	42.6	234	93.6	5.5

Applying these values of  $\mu r$  to the data given by Claassen, the values of the absorption factor were found for glancing angles  $0^\circ$ ,  $22\frac{1}{2}^\circ$ ,  $45^\circ$ ,  $67\frac{1}{2}^\circ$ , and  $90^\circ$ . Curves were then drawn giving the absorption factors for all angles between  $0^\circ$  and  $90^\circ$ , for each of the three radiations. From these curves were obtained the absorption factors by which the observed intensity values were divided. The corrected intensity values in Table I are proportional to theoretical intensity values given by the equation

$$I = \frac{1 + \cos^2 2\theta}{\sin^2 \theta \cos \theta} p F^2,$$

where  $\theta$  is the glancing angle,  $p$  the number of co-operating planes, and  $F$  the structure factor at room temperature. With the help of this equation the

\* 'Phil. Mag.', vol. 9, p. 57 (1930).

† Jönsson, 'Uppsala Univ. Årsskr.' (1928); Siegbahn, "Spektroskopie der Röntgenstrahlen," Julius Springer, Berlin (1931).



relative F values in Table III were obtained. They were reduced to a comparable scale by putting  $F_{220} = 100$  for each radiation.

This table shows some interesting features. On account of their smaller intensity, the superlattice lines  $\Sigma h^2 = 3, 4, 11, 12, 19, 20, 27, 35, 36$  are easily distinguished from the body-centred lines 8, 16, 24, 32. The superlattice lines themselves may be divided into two series, the odd reflections 3, 11, 19, 27, 35 being definitely weaker than the corresponding even reflections 4, 12, 20, 36. This distinction is to some extent obscured in Table I owing to the complications introduced by the  $\theta$  factor and the planar factor. It is shown better

Table III.—Observed F Values for Three Radiations.

Line.		Iron $K_{\alpha}$ radiation. $\lambda = 1.934$ .		Copper $K_{\alpha}$ radiation. $\lambda = 1.539$ .		Zinc $K_{\alpha}$ radiation. $\lambda = 1.434$ .	
$\Sigma h^2$ .	$hkl$ .	Relative F values.	Differences in neighbouring superlattice lines.	Relative F values.	Differences in neighbouring superlattice lines.	Relative F values.	Differences in neighbouring superlattice lines.
3	111	15	} -17 {	17	} -8 {	18	} -6 {
4	200	32		25		24	
8	220	100	} -15 {	100	} -6 {	100	} -5 {
11	311	10		11		10	
12	222	25	} -12 {	17	} -5 {	15	} -2 {
16	400	79		75		75	
19	331	6	} -7 {	9	} -2 {	8	} - {
20	420	18		14		10	
24	422	65	} - {	60	} - {	59	} - {
27	511	} 6 {		7		8	
32	440		50	} - {	47	} - {	46
35	531	4	6		-		
36	600	} 11 {	} -7 {	8	} -2 {	-	} - {
	442						

by the figures given in Table III for the differences between the F values for neighbouring odd and even lines. The table shows that *the distinction between odd and even superlattice lines is far more marked with iron radiation than with copper or zinc radiation.* We shall now discuss the explanation of this phenomenon.

It will be shown that the differences with different radiations are due to the relation of the atomic scattering factor ( $f$ ) to the wave-length  $\lambda$ .  $f$  is usually given as a function of  $\sin \theta/\lambda$  which is independent of the wave-length, but this is not strictly correct.

## II. The Atomic Scattering Factors of Aluminium, Manganese, and Copper.

It has been shown in a number of experimental investigations\* that the atomic scattering factor ( $f$ ) of an element for X-rays depends upon the wave-length of the radiation, or to put the matter more precisely, the atomic scattering factor of an element is depressed by the use of radiation whose frequency lies close to the critical K absorption frequency of the scattering element. This fact was to be expected on theoretical grounds, and is analogous to anomalous dispersion in the optical region. It has been explained with the help of a combination of classical theory and quantum mechanics by Kallmann and Mark, Kronig, and Prins.† According to Coster and Knol,‡ the theory of Prins may be expressed in the following way.

The atomic scattering factor  $f$  of an element may be regarded as consisting of two components  $f_K$  due to the K electrons, and  $f_R$  due to the L, M, etc., electrons. Now in the present experiments, the factor  $f_R$  may as a first approximation be considered to be independent of the wave-length, because we are using radiation much harder than the critical L, M, etc., absorption edges.

On the other hand, for copper and manganese, the value of  $f_K$  is very susceptible to changes in wave-length, since all three radiations used are close to the K absorption edges of these elements.

According to Coster and Knol, for radiation on the short wave-length side of the absorption edge, there is a phase-change in the contribution of the K electrons to the atomic scattering factor. This may be expressed by writing  $f_K$  as a complex quantity, thus :

$$f_K = f'_K + if''_K, \quad (2)$$

where  $i = \sqrt{-1}$ , and  $f'_K$  and  $f''_K$  are two components with a phase difference of  $\pi/2$ , the resultant of which is  $f_K$ . The component  $f'_K$  either has the same phase as  $f_R$  or differs from it by an amount  $\pi$ . The component  $f''_K$  has a phase difference  $\pi/2$  compared with  $f'_K$  and  $f_R$ .

\* Mark and Szillard, 'Z. Physik,' vol. 33, p. 688 (1925); Armstrong, 'Phys. Rev.,' vol. 34, p. 931 (1929); Wyckoff, 'Phys. Rev.,' vol. 35, pp. 215, 583, 1116 (1930); Morton, 'Phys. Rev.,' vol. 38, p. 41 (1931); Coster, Knol and Prins, 'Z. Physik,' vol. 63, p. 345 (1930); vol. 75, p. 340 (1932); Glocker and Schäfer, 'Z. Physik,' vol. 73, p. 289 (1931); Bradley and Hope, 'Proc. Roy. Soc.,' A, vol. 136, p. 272 (1932).

† Kallmann and Mark, 'Ann. Physik,' vol. 82, p. 585 (1927); Kronig and Kramers, 'Z. Physik,' vol. 48, p. 174 (1928); Prins, 'Z. Physik,' vol. 47, p. 479 (1928); Kronig, 'Phys. Z.,' vol. 30, p. 521 (1929).

‡ 'Z. Physik,' vol. 75, p. 340 (1932); 'Proc. Roy. Soc.,' A, vol. 139, p. 459 (1933).



$f'_K$  is given by the equation

$$f'_K = n_K \left\{ 1 + \frac{\log_e |x^2 - 1|}{x^2} \right\}, \quad (3)$$

where  $x = \frac{\lambda_K}{\lambda}$ ,  $\lambda_K$  being the critical absorption wave-length of the scatterer, and  $\lambda$  the wave-length of the radiation.

$f''_K$  is given by the equation

$$f''_K = \frac{\pi}{x^2} n_K. \quad (4)$$

In each of the above equations  $n_K$  represents the full effect of the K oscillators away from the region of anomalous scattering. According to Prins the most probable value of  $n_K$  is 1.3, though Kronig and Kramers gave 0.86.

For radiation on the long wave-length side of the absorption edge there is no change of phase angle, and the expression for  $f_K$  therefore simplifies to

$$f_K = n_K \left\{ 1 + \frac{\log_e |1 - x^2|}{x^2} \right\}, \quad (5)$$

where  $n_K$  and  $x$  have the same meaning as before. Taken as it stands, equation (5), like equation (3), gives values of  $f = -\infty$  at the absorption edge, but Glocker and Schäfer have shown how this may be modified by the introduction of damping terms.

The change of phase angle on the short wave-length side of the absorption edge was verified qualitatively by the experiments of Coster, Knol, and Prins with zinc blende, and the general nature of the depression of the  $f$  values near the absorption edge is well verified by all the experimental work done in this region; but no satisfactory quantitative check has yet been obtained. According to most experimenters, the scattering factor is depressed on the short wave-length side considerably more than is demanded by theory. On the contrary, Bradley and Hope found that the scattering power of iron for copper  $K_\alpha$  radiation was very little depressed. Coster and Knol have recently pointed out that a correction must be made to this result to allow for the effect of a change in phase angle. However, this correction does little to bridge the difference from the results of other investigators, as may be seen from the following table.

We have chosen what we consider to be the most probable values of the scattering factors of copper and manganese, based on the experimental work of Bradley and Hope. They compared the values of the atomic scattering factor of iron for different radiations at the same value of  $\sin \theta/\lambda$ . For both

Table IV.—The Atomic Scattering Factor of Iron ( $f_{110}$ ).

Radiation.	$\lambda/\lambda_K$ .	Glocker and Schäfer*		Wyckoff.†	Bradley and Hope.	Calculated from equations (3), (4), (5).
Mo $K_\alpha$ .....	0.41	16.3	(17.1)	16.3	17.2	17.55
Cu $K_\alpha$ .....	0.89	9.4	(11.6)	11.8	16.1	16.3
					(corrected)	
Ni $K_\alpha$ .....	0.95	8.0	—	10.1	—	—
Co $K_\alpha$ .....	1.01	—	—	—	14.1	12.6
Fe $K_\alpha$ .....	1.10	11.9	(13.5)	13.8	15.7	14.5
Cr $K_\alpha$ .....	1.31	12.7	—	—	17.2	15.25

\* Glocker and Schäfer have recently amended these values, and in a private communication to one of the authors they give values more nearly in agreement with those of Wyckoff. These are given in brackets.

† Corrected for temperature factor.

Cobalt and iron radiations the scattering factor was found to be depressed below that for molybdenum radiation by an amount which was almost independent of  $\sin \theta/\lambda$ . This is to be expected on theoretical grounds. The depressions are due to changes in the contributions of the K electrons to the atomic scattering factor for different values of  $\lambda/\lambda_K$ . These depend only on  $n_K$  which is almost independent of  $\sin \theta/\lambda$ .

For copper  $K_\alpha$  radiation, according to Coster and Knol, the difference in scattering factor should be greater as the value of  $\sin \theta/\lambda$  increases, owing to the fact that  $f_K$  is a complex quantity. However, we may split up the atomic scattering factor into its two components, a real component ( $f_R + f'_K$ ) and an imaginary component,  $f''_K$  which differs in phase by  $\pi/2$ . At all values of  $\sin \theta/\lambda$ , ( $f_R + f'_K$ ) should be depressed by the same amount. It is therefore possible to obtain for each radiation a characteristic value of the depression of the "real" component of the  $f$  curve of iron, which is independent of  $\sin \theta/\lambda$ .

The depression in  $f$  in the neighbourhood of the K absorption edge is due to a variation in the contribution of the K electrons to the total  $f$  value of the atom. Whether we use a combination of classical theory and quantum theory (as Prins has) or a purely wave-mechanical theory,\* the variation in the contribution of the K electrons to the total value for the atom is a function of  $\lambda/\lambda_K$ .

It follows from this result that the anomalous dispersion by different elements can be deduced from experiments on one element only, provided the results

\* We are indebted to Dr. Williams of this University for discussing this matter with us.



are expressed in terms of  $\lambda/\lambda_K$ . Experiments are now being undertaken to test the validity of this generalization, the results of which will be communicated in due course.

In fig. 4 the depressions in the observed  $f$  values for iron are plotted against the values of  $\lambda/\lambda_K$ ,  $\lambda$  being the wave-length of the radiations used (Mo, Cu, Co, Fe, Cr characteristic  $K_\alpha$  radiations), and  $\lambda_K$  the wave-length of the K

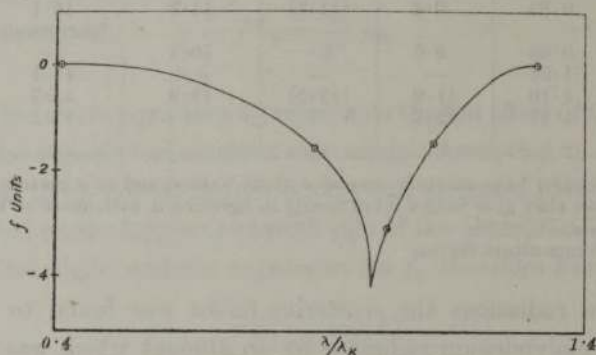


FIG. 4.—Depression of  $f$  curves in the region of the K absorption edge.  $\odot$  Points from experiments on FeAl (Bradley and Hope) giving the difference between the normal  $f$  values and the values found near the absorption edge. For Cu radiation the value plotted is not  $f$  but  $f_R + f'_K$ .  $f''_K$  is calculated separately from the formula

$$f''_K = \frac{\pi}{x^2} n_K.$$

absorption edge of iron. The values for molybdenum radiation are taken as zero. In this figure the values of the depression at some distance from the absorption edge approach zero, and the biggest values of the depression are in the immediate neighbourhood of the K edge. Plotted as a function of  $\lambda/\lambda_K$ , theory indicates that the values represented on this curve should be universal. They represent the amounts to be subtracted from the normal  $f$  values where the frequency of the radiation is comparable with the critical absorption frequency.

In order to obtain the value of the atomic scattering factor for a given element with a given radiation for a given value of  $\sin \theta/\lambda$ , we first take the "normal" value of the atomic scattering factor of the element for the required value of  $\sin \theta/\lambda$ , and then subtract an amount read off from this curve, fig. 4, to allow for the anomalous effects of the K absorption edge on  $f_K$ . Then we calculate the amount of  $f''_K$  from equation (4), assuming  $n_K = 1.3$ , and introduce a separate term into the calculations to allow for the effect of  $f''_K$  when

$\lambda/\lambda_K < 1$ . An illustration will show how simple the procedure can be. To find  $f_{Mn} - f_{Al}$  for copper  $K_\alpha$  radiation we have

$$F = \sqrt{(f_{Mn} \text{ normal} - f_{Mn} \text{ depression} - f_{Al})^2 + f''_{K^2}} \quad (6)$$

Table V contains the necessary data for the evaluation of this expression, for the Heusler alloy.

Table V.—Depression in  $f$  Curve, due to Anomalous Dispersion.

Scattering elements.	$\lambda_K$ .	Zinc $K_\alpha$ radiation. $\lambda = 1.434$ .	Copper $K_\alpha$ radiation. $\lambda = 1.539$ .	Iron $K_\alpha$ radiation. $\lambda = 1.934$ .
Al 13 .....	7.936	0	0	0
Mn 25 .....	1.892	1.0	1.0	3
Cu 29 .....	1.377	2.5	1.5	0

Substituting in equation (6),

$$F = \sqrt{(f_{Mn} \text{ normal} - f_{Al} - 1.0)^2 + 2.7^2}$$

The normal  $f$  curves of aluminium, manganese, and copper were obtained from a paper by James and Brindley.\* The aluminium values were calculated by Hartree's method of self-consistent fields; for copper an approximate curve was obtained by the same method; for manganese, the Thomas values were used. It was shown by Bradley and Hope that the Thomas curve for iron gave an excellent agreement for molybdenum radiation, and since manganese is the next element to iron and does not differ greatly in atomic volume, it seems fairly safe to use the Thomas curve here, though, of course, it is probably less accurate than the other two calculated by Hartree's method.

It is now possible to understand the differences in the powder photographs taken with zinc, copper, and iron radiations. As Table V shows, the atomic scattering factor of manganese with iron radiation is three units less than normal, whereas that of copper with iron radiation is practically normal. Hence the difference in scattering power between copper and manganese is *three units greater* than normal. On the other hand, with zinc radiation the scattering power of copper is depressed more than that of manganese, so that the difference in scattering power between copper and manganese is now *1.5 units less* than normal. Thus iron radiation emphasizes the difference in scattering power between copper and manganese, whereas zinc radiation

\* 'Phil. Mag.,' vol. 12, p. 81 (1931); 'Z. Kristallog.,' vol. 78, p. 470 (1931).



minimizes the difference. This fact naturally leads to differences in the intensities of the weaker reflections, where copper and manganese work in opposite directions. As we shall see later, the figures given in Table V provide not merely a qualitative explanation, but ultimately give a perfect quantitative explanation of all the observed intensities (Table VII).

On the other hand, if we had used the data of Glocker and Schäfer or of Wyckoff, we should have been led to the conclusion that the scattering powers of copper and manganese with iron radiation ought not to be appreciably different from those with copper or zinc radiation. The different results obtained with different radiations prove that this is impossible. The theoretical expressions (equations (3), (4), and (5)) predict a difference between the scattering powers of copper and manganese for the different radiations employed, but do not explain the observed numerical values as well as our empirical values from the iron-aluminium experiments. Possibly more accurate results would be obtained if this theory took account of the variation in the contribution of the L electrons as well as the K electrons. The empirical curve, given in fig. 4, automatically makes this allowance, and partly for this reason should give accurate  $f$  values, if the experiments of Bradley and Hope are a sufficient basis for the curve. It is expected that new data will shortly become available, giving more points on the curve.

### III. Possible Structure for the Heusler Alloy.

The unit cell contains 16 atoms with the co-ordinates:—

A	.....	0 0 0,	$0 \frac{1}{2} \frac{1}{2},$	$\frac{1}{2} 0 \frac{1}{2},$	$\frac{1}{2} \frac{1}{2} 0$
B	.....	$\frac{1}{4} \frac{1}{4} \frac{1}{4},$	$\frac{1}{4} \frac{3}{4} \frac{3}{4},$	$\frac{3}{4} \frac{1}{4} \frac{3}{4},$	$\frac{3}{4} \frac{3}{4} \frac{1}{4}$
C	.....	$\frac{1}{2} \frac{1}{2} \frac{1}{2},$	$\frac{1}{2} 0 0,$	$0 \frac{1}{2} 0,$	$0 0 \frac{1}{2}$
D	.....	$\frac{3}{4} \frac{3}{4} \frac{3}{4},$	$\frac{3}{4} \frac{1}{4} \frac{1}{4},$	$\frac{1}{4} \frac{3}{4} \frac{1}{4},$	$\frac{1}{4} \frac{1}{4} \frac{3}{4}$

Symmetry considerations divide the atoms into the four sets A, B, C, D, as shown in fig. 2. The problem is to find which of these positions are occupied by copper, aluminium, and manganese atoms respectively. The data of Table III point the way to a solution.

Three facts must be explained:—

- (1) The existence of three series of reflections, one strong series of lines [(1) 220, 400, 422, 440], and two weak series of superlattice lines

$$\left[ (2) 200, 222, 420, 600 \right], \left[ (3) 111, 311, 331, 511, 531 \right].$$

- (2) The superlattice lines of series (3) are definitely weaker than those of series (2).
- (3) The difference in intensity of the two series of superlattice lines depends on the wave-length of the radiation, being greatest for iron radiation and least for zinc radiation.

Let the scattering powers in the four groups be  $f_a$ ,  $f_b$ ,  $f_c$ , and  $f_d$  respectively. Then the structure factors for planes of types (1), (2), (3) may be written in the following way:—

$$\begin{aligned} (1) \quad f &= f_a + f_b + f_c + f_d \\ (2) \quad f &= (f_a + f_c) - (f_b + f_d) \\ (3) \quad f &= \sqrt{(f_c - f_a)^2 + (f_d - f_b)^2}. \end{aligned}$$

From these equations it may be seen that the presence of reflections of both types (2) and (3) requires one group to be appreciably different in scattering power from the other three. Since copper and manganese are not very different in scattering power, this condition is equivalent to a requirement that most if not all the aluminium atoms should be sorted out into one group, say B.

If the atoms in groups A, C, D were equivalent in scattering power, reflections of types (2) and (3) would be equally strong. This is not so. The greater intensity of type (2) reflections shows that the scattering power of D groups is intermediate between those of A and C on the one hand and B on the other. This admits of two interpretations: either manganese atoms go into D positions, or the aluminium atoms are not completely sorted out into B positions, a minority of the aluminium atoms being found in D positions.

The second alternative would be analogous to the iron aluminium alloys\* containing a little more than the correct amount of aluminium to satisfy the formula  $\text{Fe}_3\text{Al}$ . Here most of the aluminium atoms occupy position B, but a certain proportion move over to position D, leaving B without its full complement of aluminium atoms.

To distinguish between the two alternatives, it is necessary to make use of the fact that the intensities of the two sets of superlattice lines differ considerably with different radiations (see Table III). This could not be explained by a partial distribution of aluminium between positions B and D. It can, however, be explained by placing manganese atoms in D and aluminium atoms in B. This distribution gives structure factors  $2\text{Cu} - (\text{Mn} + \text{Al})$  and  $(\text{Mn} - \text{Al})$  for types (2) and (3) respectively. The difference is  $2(\text{Cu} - \text{Mn})$ . As we have shown in a previous paragraph, the scattering power of copper

\* Bradley and Jay, 'Proc. Roy. Soc.,' A, vol. 136, p. 210 (1932).



exceeds that of manganese more with iron radiation than with copper and zinc radiations. With this structure, we should therefore expect that the intensity differences between reflections of type (2) and (3) would be greatest with iron radiation and least with zinc radiation, which is in complete accordance with the facts.

The above arguments show that most of the aluminium atoms are in position B and most of the manganese atoms are in position D, but the sorting out of the atoms cannot be complete, because the composition of the alloy does not correspond exactly to the formula  $\text{Cu}_2\text{MnAl}$ . In order to decide the exact arrangement, a quantitative test is necessary. Before comparing the observed intensities with the calculated values for the most probable arrangement, we shall first give calculations for three different arrangements of manganese atoms with the ideal composition  $\text{Cu}_2\text{MnAl}$ . It will be seen that the differences between the intensities of the superlattice lines in the three cases are so large that it is possible to be quite sure of the ultimate solution.

The three arrangements considered first are:—

- (i) Mn in D, Cu in A and C, Al in B.
- (ii) Mn and Cu at random in A, C, and D, Al in B.
- (iii) Mn in A, Cu in C and D, Al in B.

Table VI.—Comparison of Observed and Calculated Intensities for Three Different Structures.

Line.		Iron $K_{\alpha}$ radiation. $\lambda = 1.934$ .				Copper $K_{\alpha}$ radiation. $\lambda = 1.539$ .			
$\Sigma h^2$ .	$hkl$ .	Observed with temperature correction.	Calculated.			Observed with temperature correction.	Calculated.		
			i.	ii.	iii.		i.	ii.	iii.
3	111	14	10	27	48.5	33	28	43	59
4	200	36	49	14	5	39.5	51	23	14
8	220	340	354	354	354	600	593	593	593
11	311	4.5	2	10	22	11	9.5	17	26
12	222	9.5	12	3	0.5	8	12	5	3
16	400	57	56	56	56	88	90	90	90
19	331	1.5	1	4	9.5	4	3.5	6	8.5
20	420	11.5	17	4	0.5	10	12	5	2.5
24	422	156	148	148	148	173	167	167	167
27	{ 511 333 }	{ 2	1	4.5	11	2.5	3	4	5.5
32	440	97	95	95	95	51	54	54	54
35	531	3.5	2.5	12.5	30	3.5	3.5	4	5.5
36	{ 600 442 }	{ 29	46	10	2	4.5	5	2.5	2

In order to make the observed intensities comparable with the calculated values, they must be reduced to the same scale. This process is complicated because the observed values are found at room temperature, whereas the calculated values apply only at the absolute zero of temperature. This causes the observed intensities to fall off too quickly with increasing values of  $\sin \theta/\lambda$ . The observed values should be related to the calculated values in the following

ray :

$$I_{\text{obs.}} = I_{\text{calc.}} K e^{-\frac{B \sin^2 \theta}{\lambda^2}},$$

where  $\lambda$  is the wave-length and  $\theta$  the glancing angle.  $B$  is a physical constant which is the same for all radiations.  $K$  is arbitrary and differs for each experiment, depending on the experimental conditions. The scales of the observed values are adjusted by choosing values of  $K$  and  $B$  to give the best measure of agreement between the observed and calculated reflections for planes 220, 400, 422, and 440, the values of which are independent of the atomic arrangement. It was found that the best agreement between observed and calculated values was obtained by putting  $B = 3$ .

Table VI includes results from iron and copper radiations. The zinc values are not included as the difference in the scattering powers of copper and manganese is too small to give decisive results. It can be seen from this table that almost all the observed intensity values of the superlattice lines lie between the calculated values for structure (i) and structure (ii). Structure (iii) is, therefore, ruled out.

The obvious interpretation of this result is that structure (i) is essentially correct, but since there are too few manganese atoms to fill the whole of the D positions some of the manganese has been replaced by copper. This has the effect of reducing the difference in scattering power between A and C on the one hand and D on the other. The formula for the alloy may be written as  $\text{Cu}_2(\text{MnCu})\text{Al}$ . It must, however, be taken into account that there is a small proportion of aluminium atoms in excess. This must either replace copper in A and C or manganese in D. Good agreement with the observed intensities can only be obtained if it is supposed that the excess of aluminium is equally distributed between positions A, C, and D. The most probable atomic distribution is as follows :—

A atoms : 0.95 copper, 0.05 aluminium.

B atoms : All aluminium.

C atoms : 0.95 copper, 0.05 aluminium.

D atoms : 0.3 copper, 0.65 manganese, 0.05 aluminium.



The calculated intensities for this structure are compared with the observed values in Table VII. The scale has again been fixed to give the best agreement for the strong reflections, which depend only on the composition and not on the manner in which the atoms of different kinds are distributed. The intensities of the superlattice lines are thus obtained on an absolute scale, and the close agreement with the calculated values can therefore be taken as a conclusive proof that both the structure is correct and also that the empirical rule for calculating  $f$  values in the neighbourhood of the K absorption edge is reliable.

Table VII.—Comparison of the Observed and Calculated Intensities for the Most Probable Structure.

Line.		Iron $K_{\alpha}$ radiation. $\lambda = 1.934$ .		Copper $K_{\alpha}$ radiation. $\lambda = 1.539$ .		Zinc $K_{\alpha}$ radiation. $\lambda = 1.434$ .	
$\Sigma h^2$ .	$hkl$ .	Observed.	Calculated.	Observed.	Calculated.	Observed.	Calculated.
3	111	15	15	32.5	30	37	40
4	200	37.5	37	38.5	39	39	36
8	220	353	364	587	589	655	647
11	311	5	5	11	11.5	10	11
12	222	10	8.5	8	9	7	8
16	400	59	57	86	87	95	95
19	331	1.5	2	4	4	3	4
20	420	12	12	9.5	9.5	6	7
24	422	161	153	169	164	172	171
27	{ 511 333 }	{ 2 2 }	{ 2 2 }	{ 2.5 3 }	{ 3 4 }	{ 4 3 }	{ 3 3 }
32	440	101	98	50	52	49	50
35	531	3.5	5.5	3.5	3	—	—
36	{ 600 442 }	{ 30 30 }	{ 32 32 }	{ 4.5 4.5 }	{ 3.5 3.5 }	{ — — }	{ — — }

In conclusion, the authors thank Professor W. L. Bragg, F.R.S., for his kind interest in the work, which was carried out in the Physical Laboratories of the University of Manchester.

#### Summary.

In an investigation of the ferromagnetic alloys of copper, manganese, and aluminium an alloy was found which showed an almost complete change of crystal structure due to heat treatment. Drillings of this alloy, which had been annealed at  $500^{\circ}$  for several hours and cooled slowly to room temperature, were found to have the  $\delta$  copper aluminium ( $\text{Cu}_9\text{Al}_4$ ) type of structure. The formula may be written as  $(\text{CuMn})_9\text{Al}_4$ , the atoms occupying the same positions as in  $\text{Cu}_9\text{Al}_4$ . The annealed and slowly cooled alloy is non-magnetic, but on

quenching from 800° C. it becomes strongly ferromagnetic. The structure is now entirely body-centred cubic, with a face-centred superlattice.

A quantitative X-ray examination of the ferromagnetic alloy showed the utility of a new method for distinguishing between elements of almost equal scattering power. On comparing X-ray powder photographs of the same specimen made with radiations from iron, copper, and zinc anticathodes, it was found that the relative intensities of the weaker reflections varied with the wave-length of the radiation. This fact made it possible to distinguish the manganese atoms from the copper atoms, which would not have been possible if results from only one radiation had been available. The difference between the atomic scattering factors of copper and manganese which is very small with zinc radiation becomes fairly large with iron radiation.

The ideal structure of the ferromagnetic alloy would be :—

Cu	.....	0 0 0	$0 \frac{1}{2} \frac{1}{2}$	$\frac{1}{2} 0 \frac{1}{2}$	$\frac{1}{2} \frac{1}{2} 0$
		$\frac{1}{2} \frac{1}{2} \frac{1}{2}$	$\frac{1}{2} 0 0$	$0 \frac{1}{2} 0$	$0 0 \frac{1}{2}$
Al	.....	$\frac{1}{4} \frac{1}{4} \frac{1}{4}$	$\frac{1}{4} \frac{3}{4} \frac{3}{4}$	$\frac{3}{4} \frac{1}{4} \frac{3}{4}$	$\frac{3}{4} \frac{3}{4} \frac{1}{4}$
Mn	.....	$\frac{3}{4} \frac{3}{4} \frac{3}{4}$	$\frac{3}{4} \frac{1}{4} \frac{1}{4}$	$\frac{1}{4} \frac{3}{4} \frac{1}{4}$	$\frac{1}{4} \frac{1}{4} \frac{3}{4}$

In the specimen examined there was a deficit of manganese atoms. The alloy was nevertheless homogeneous, some copper taking the place of the missing manganese atoms. The aluminium atoms in excess were distributed equally in the positions normally occupied by copper and manganese.